J O U R N A L O F
**Ceramic**
**Processing Research**

# Coating of Si₃N₄ with HAp via atomic layer deposition

**Seniz R. Kushan Akin***

*Department of Materials Science and Engineering, Cankaya University, Ankara, Turkey*

**Silicon nitride (Si₃N₄) is an attractive implant material, particularly in orthopedic surgery. Although it has only been on the market for spinal fusion surgery requirements so far, it is also a promising candidate for other implant applications where load-bearing is crucial. In this study, we aimed to examine the potential of making the material surface more advantageous for various implant applications by coating it with a very thin hydroxyapatite (HAp) layer using the atomic layer deposition (ALD) method. This was done to improve the material's bioactivity without sacrificing its mechanical properties. Characterization results showed that using a 3:1 CaO:PO4 ALD cycle ratio resulted in the formation of very fine crystalline HAp after heat treatment at 500 °C. The bioactivity assessment made by immersing the coated film in SBF revealed HAp formation on the surface, and it was observed that the bioactivity of this surface improved compared to the uncoated one.**

**Keywords: Silicon nitride, Atomic layer deposition, Hydroxyapatite.**

## Introduction

Si₃N₄ ceramics have great potential as biomedical implant materials due to their favorable mechanical and biological properties. In addition to the high hardness and wear resistance brought by its high covalency, Si₃N₄ has relatively high fracture toughness among ceramic materials, which is strongly related to the presence of highly anisotropic rod-like β-Si₃N₄ grains in the microstructure [1-4]. Si₃N₄'s so-called "bioinert" behavior makes it attractive as a biomaterial compared to routinely used oxide bioceramics like Al₂O₃, ZrO₂, and their composites. One of the principal reasons why it is compatible as a biomaterial is based on its biologically accepted elements. N is a natural component of the human body, and Si ion release has been shown to contribute to osteoblast formation and inhibit osteoclast activity [5]. Studies on Si₃N₄ have shown no cytotoxicity [6], decreased bacteria activity compared to titanium and polyether ether ketone (PEEK) [7, 8], and no inhibition of bone growth around implants [9]. Moreover, its absence of artifacts on radiograms, CT, and MRI images with standard imaging techniques makes this material more attractive for clinical use [10].

In some recent studies, it was shown that Si₃N₄ interacts with the surrounding cells in the microscopic domain of biomolecular interfaces, so it can be regarded as a "bioactive" material [11, 12]. Due to its unique surface chemistry, Si₃N₄ has a certain interaction with the surrounding tissue, which yields a conflict in defining it as a bioinert material. However, this bioactivity is not as described by IUPAC [13] like bioglass. Moreover, its degree of biocompatibility or osseointegration can still be improved to prevent failure in the host body through additional surface modification techniques.

Since it is really the surface that reacts with the host tissue, numerous surface-altering techniques are being studied to enhance performance in a biological environment while retaining the bulk properties of Si₃N₄. Some of these surface studies include surface modification techniques [14, 15] and surface overcoatings like grafting [16] or thin film deposition [17-19]. The overcoated layer is generally expected to be as thin as possible to have increased mechanical performance through better bonding strength and reduced residual stresses [20]. Additionally, thicker coatings are more susceptible to delamination and cracking. For this reason, a coating thickness of 3-10 Å is ideally preferred [21], but coating the surface of Si₃N₄ at the atomic level has not yet been reported. Thicknesses ranging from 10-100 nm have been practically obtained so far.

Calcium phosphate-based ceramics are commonly used coatings for orthopedic prostheses, and hydroxyapatite (HAp), Ca₁₀(PO₄)₆(OH)₂, is the most widely used among them since it quickly integrates with bones and promotes the growth of new bones [22]. It has a hexagonal crystal structure, just like Si₃N₄. The atomic ratio of Ca/P is 1.67, which is the ratio of these components in natural bones. Currently, it is a versatile biomaterial and also has huge development potential [23-26]. However, the brittle nature of HAp and its relatively poor mechanical properties, especially its low

*Corresponding author:
 Tel : +90 312 233 1502
 Fax: +90 312 233 1026
 E-mail: senizakin@cankaya.edu.tr

fracture toughness, limit its use, making it more attractive as a thin coating material than for direct use in bulk form.

Thicknesses obtained via different techniques for the deposition of HAp coating were summarized by Harun et.al. and different coating/substrate materials, coating techniques, coating thickness and adhesion quality on metallic biomaterials were discussed [27]. Some studies have successfully coated $Si_3N_4$ ceramics with HAp using biomimetic or sol-gel methods [18, 28, 29]. However, these methods do not result in an atomic level coating layer, which may have a negative impact on the mechanical properties of $Si_3N_4$ ceramics.

The current study focuses on an alternative HAp coating technique, atomic layer deposition (ALD), on $Si_3N_4$ substrates. The goal is to create a conformal and chemically homogeneous coating with high sensitivity at the Angstrom level. As far as the authors are aware, this is the first time this deposition method has been applied and characterized on $Si_3N_4$ substrates. However, there have been several studies on HAp coating using ALD processes with different procedures and on different substrates.

In 2009, Putkonen et al. used Ca(thd)$_2$ (thd = 2,2,6,6-tetramethyl-3,5-heptanedione) and (CH$_3$O)$_3$PO (Merck N 98%) as calcium and phosphorous precursors of ALD process, respectively, to produce HAp on Si and Corning substrates. The resulting coatings were characterized for crystallinity, stoichiometry, possible impurities, and surface morphology [30]. In Holopainen's 2014 study, the substrate was coated with $CaCO_3$ using the ALD process, and then converted to hydroxyapatite using a diammonium hydrogen phosphate (DAP) solution [31]. In another study by the same group, nanocrystalline hydroxyapatite thin films were fabricated on titanium using the same process in 2019 [32].

The current study investigates the potential for atomic layer HAp coating using suitable precursors with a simpler process than the previously reported methods. The goal is to improve the bioactivity of $Si_3N_4$ ceramics without negatively impacting their mechanical properties.

## Materials and Methods

### Materials

The $Si_3N_4$ substrates used in this study were supplied by a commercial company (MDA Advanced Ceramics Ltd., Turkey). They were sintered via gas pressure sintering with densification additives, similar to the methods previously reported [33]. While producing these samples, $Si_3N_4$ powder (Ube SN E-10, Ube City, Japan) was mixed with sintering additives and cold-pressed at room temperature into square-shaped samples. Then samples were sintered under nitrogen via gas pressure sintering at a temperature in excess of 1700 °C. Substrates were used in the as-received (as-fired)

condition without polishing. Ultrasonic surface cleaning was performed by acetone, ethanol and deionized water (each for 15 min.) before coating. Additionally, Si wafer substrates were also coated to be used for ease of some analysis/characterization of the deposited films.

### Atomic layer deposition

ALD process is based on the sequential use of self-terminating surface reactions. All the chemicals related to the ALD process were provided by Veeco. $Si_3N_4$ samples placed in the ALD chamber were all 10×10×6 mm in size. The films were deposited onto the $Si_3N_4$ substrates using calciumformadinate and ozone for CaO deposition and TMPO and ozone for PO$_4$, with $H_2O$ and $O_3$ as co-reactants to compare the effect of co-reactant on uniformity and stability in air films. In order to obtain the exact stoichiometry, 2 different ALD cycle ratios were applied; 3:1 and 2:1 by means of CaO:PO$_4$. The thin film was grown at a temperature of 250 °C and ~50 nm thickness of the film was obtained after 12 hours.

### Heat Treatment

Coating was amorphous right after the ALD process, therefore heat treatment was conducted at 500 °C for 1 h under atmospheric conditions to achieve a crystalline coating layer [34].

### Characterization
#### SEM/EDX Analysis

The surfaces of the samples were examined with a field-emission gun scanning electron microscope (FE-SEM) (Hitachi S-4800) equipped with energy dispersive x-ray spectroscopy (EDX) using the secondary electron imaging mode. Samples were Pt coated before observation.

#### Thin Film XRD Analysis

X-ray diffraction (XRD) method was used to determine the crystallinity of deposited films. A Rigaku Miniflex system equipped with Cu Kα radiation (0.154 nm) was used. The diffraction tests were performed for diffraction angle (2θ) between 20° and 80° at a scan rate of 1°/min

#### XPS Analysis

Electronic characteristics and surface chemical analyses of the films were performed by X-ray photoelectron spectroscopy (XPS). XPS analyses were conducted using a monochromatic Al Kα X- 42 ray source (1486.6 eV) with a PHI 5000 VersaProbe.

### Bioactivity Test

SBF was prepared by adapting the recipe specified by Kokubo et al. [35]. Samples were cleaned individually (15 min each) with acetone, ethanol and deionized water before being tested for bioactivity in simulated body fluid (SBF) and soaked in SBF for 14 days at a

constant temperature of 36.5±0.5 °C. The SBF solution was refreshed every other day to stabilize the ion concentration. At the end of 14 days, the samples were washed in distilled water to remove any residual salts on the surface and dried at room temperature. The bioactivities of the surfaces were evaluated via Scanning Electron Microscope (SEM) by examining the HAp formation.

## Results and Discussion

ALD, is a thin film coating method that can uniformly deposit films on both smooth and rough, three-dimensional surfaces. In ALD, the substrate is exposed to one gaseous precursor, which chemisorbs on accessible sites on the surface. When no more available sites are present, the reaction self-terminates and excess precursor is purged out of the chamber. Then, the second precursor is introduced and reacts with the available sites created by the first precursor until saturation and self-termination, resulting in a layer of binary structure [36]. In this study, calciumformadinate and ozone were used for CaO deposition and TMPO and ozone were used for $PO_4$ deposition, with $H_2O$ and $O_3$ as co-reactants.

Microscopic examination of the surface using FE-SEM revealed that a typical plate-like hydroxyapatite (HAp) crystal structure could not be identified from the top view. However, energy-dispersive X-ray spectroscopy (EDX) analysis of Si wafer substrates, which were coated and heat-treated under the same conditions to facilitate the same analysis/characterization of the deposited films, provided insight into the stoichiometry obtained. According to the EDX results, when the Ca/P ratio was examined, the Ca/P atom ratio was very close to the atomic ratio of HAp (1.667) in samples with a 3:1 ratio of $CaO:PO_4$ precursors in the ALD process, making it more promising for apatite formation. The Ca/P atomic ratio was 1.37 for the coated samples with a 2:1 $CaO:PO_4$ precursor ratio.

The calcium to phosphorus elemental ratios of the deposited $Si_3N_4$ specimens were analyzed using XPS for a more precise examination (Fig. 2). The XPS survey spectra of the 3:1 and 2:1 $CaO:PO_4$ ALD cycles showed similar contributions, but a minor fluorine contamination was observed in the 3:1 ratio sample. Based on this data analysis, the elemental ratios of calcium to phosphorus were determined to be approximately 1.3 and 1.4 for the 3:1 and 2:1 $CaO:PO_4$ ALD cycles, respectively. It was observed that the results of the Ca/P ratio obtained with XPS did not fully overlap with the results obtained with EDX in terms of HAp formation for the 3:1 $CaO:PO_4$ ALD cycles, although the results were quite similar for the 2:1 ratio. According to these results, the films did not consist of stoichiometric hydroxyapatite but of a Ca-deficient type of apatite.

Thin film XRD patterns were analyzed to determine the crystallinity of the films and to observe the existence of the HAp phase (Fig. 3). According to the XRD spectra, the amorphous film obtained at the end of the ALD process was fully converted into a crystalline form by heat treatment. The diffraction angles varying between 20° and 60 revealed that the coating with a 3:1
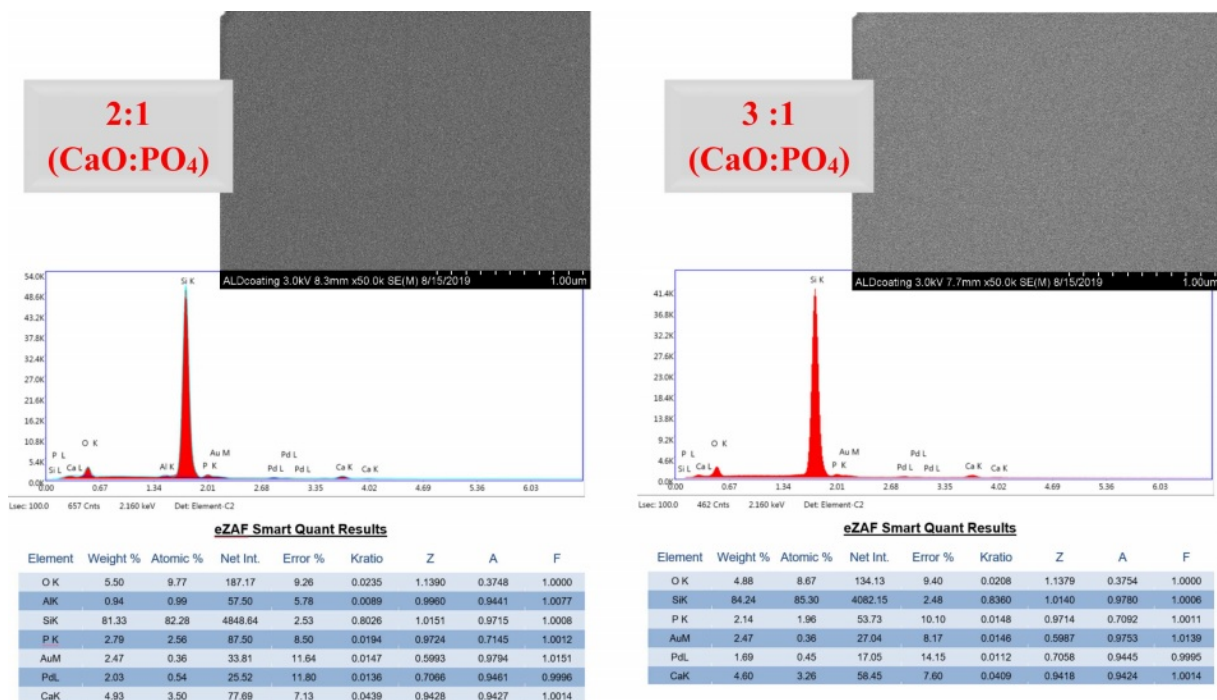


**2:1 (CaO:PO₄) — eZAF Smart Quant Results**

| Element | Weight % | Atomic % | Net Int. | Error % | Kratio | Z | A | F |
|---|---|---|---|---|---|---|---|---|
| O K | 5.50 | 9.77 | 187.17 | 9.26 | 0.0235 | 1.1390 | 0.3748 | 1.0000 |
| Al K | 0.94 | 0.99 | 57.50 | 5.78 | 0.0089 | 0.9960 | 0.9441 | 1.0077 |
| Si K | 81.33 | 82.28 | 4848.64 | 2.53 | 0.8026 | 1.0151 | 0.9715 | 1.0006 |
| P K | 2.79 | 2.56 | 87.50 | 8.50 | 0.0194 | 0.9724 | 0.7145 | 1.0012 |
| Au M | 2.47 | 0.36 | 33.81 | 11.64 | 0.0147 | 0.5993 | 0.9794 | 1.0151 |
| Pd L | 2.03 | 0.54 | 25.52 | 11.80 | 0.0136 | 0.7066 | 0.9461 | 0.9996 |
| Ca K | 4.93 | 3.50 | 77.69 | 7.13 | 0.0439 | 0.9428 | 0.9427 | 1.0014 |

**3:1 (CaO:PO₄) — eZAF Smart Quant Results**

| Element | Weight % | Atomic % | Net Int. | Error % | Kratio | Z | A | F |
|---|---|---|---|---|---|---|---|---|
| O K | 4.88 | 8.67 | 134.13 | 9.40 | 0.0208 | 1.1379 | 0.3754 | 1.0000 |
| Si K | 84.24 | 85.30 | 4082.15 | 2.48 | 0.8360 | 1.0140 | 0.9780 | 1.0006 |
| P K | 2.14 | 1.96 | 53.73 | 10.10 | 0.0148 | 0.9714 | 0.7092 | 1.0011 |
| Au M | 2.47 | 0.36 | 27.04 | 8.17 | 0.0146 | 0.5987 | 0.9753 | 1.0139 |
| Pd L | 1.69 | 0.45 | 17.05 | 14.15 | 0.0112 | 0.7058 | 0.9445 | 0.9995 |
| Ca K | 4.60 | 3.26 | 58.45 | 7.60 | 0.0409 | 0.9418 | 0.9424 | 1.0014 |

**Fig. 1.** SEI and EDX results of XRD patterns of coated (followed by annealing) Si substrates after atomic layer deposition.
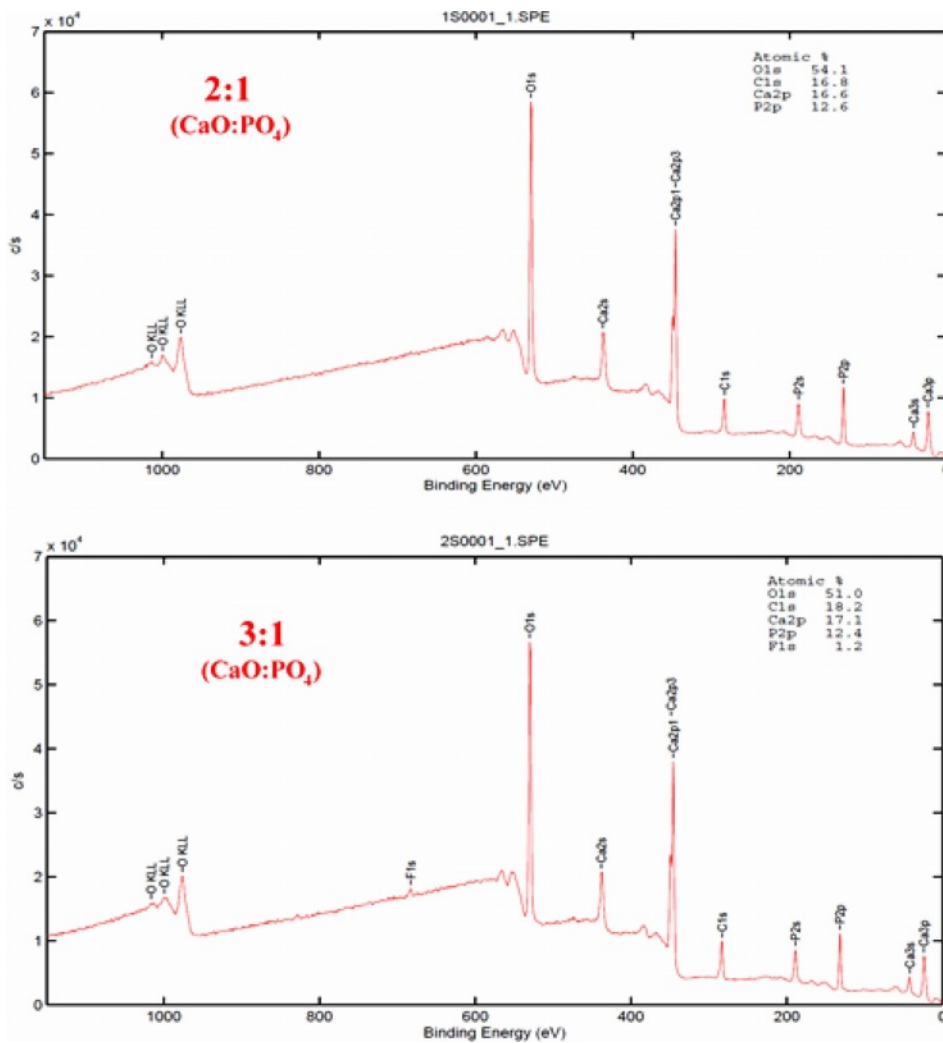
**Fig. 2.** XPS spectra of the ALD coatings deposited on Si$_3$N$_4$ substrates.

CaO:PO$_4$ conversion ratio is more promising in terms of HAp yield. The underlying Si$_3$N$_4$ phase was confirmed by the standard Si$_3$N$_4$ peaks matching. The dashed red lines in Fig. 3 represent the pattern obtained from the XRD examination of the uncoated surface. The intensity values obtained from the uncoated pattern are quite high as the examination is carried out throughout the bulk material. However, in the coated material, the intensity value is lower since the information comes from a thin surface layer. Except for the peaks matching Si$_3$N$_4$, the other peaks were observed to be compatible with HAp (shown in circles in Fig. 3). Despite the decrease in intensity values for Si$_3$N$_4$ peaks, it is noteworthy that the thin HAp phase in the coated materials was observed. Not all the diffraction peaks of the HAp phase are distinctive since the coating is too thin. This is because the crystalline structures of the films are formed by grains that can be oriented either randomly or with some degree of preferred orientation [37]. The XRD results indicate that the HAp phase was achieved by the ALD process
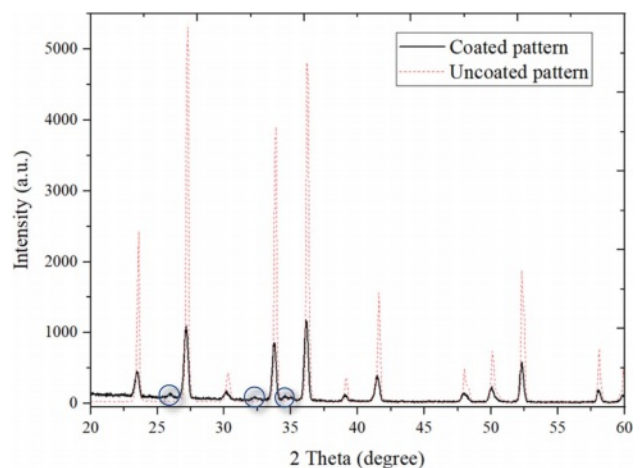


**Fig. 3.** XRD patterns of uncoated and coated (3:1 of CaO:PO$_4$ cycle followed by annealing at 500 °C).

and could be crystallized after annealing at 500 °C since well-defined peak shapes were obtained.

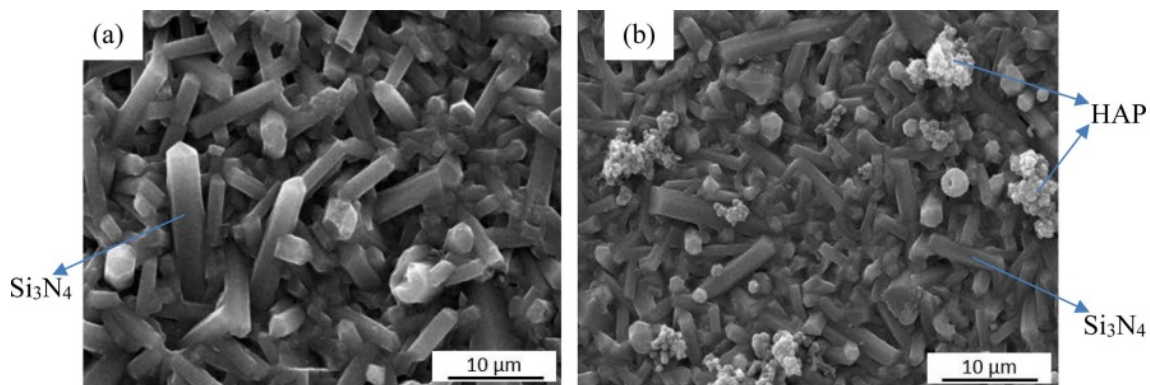To compare the effect of ALD coating on the

**Fig. 4.** SI images of the (a) uncoated and (b) coated (3:1 of CaO:PO$_4$ cycle followed by annealing at 500 °C) Si$_3$N$_4$ samples after being soaked in SBF for 14 days.

bioactivity of the surface and its apatite forming ability [35], the coated and uncoated samples were immersed in SBF for 14 days and examined with secondary electrons (SE) (Fig. 4). As shown in Fig. 4a and 4b, the typical rod-like microstructure of β-Si$_3$N$_4$ grains was observed in both coated and uncoated substrates. However, dispersed globules of precipitated HAp were observed on some parts of the ALD-coated samples, similar to the HAp coatings observed elsewhere [36]. Since the ALD coating is applied directly to the as-produced sample and there is a very thin coating layer on the surface due to the nature of the applied process, this morphology was observed as an "island" after nucleation only in certain regions with a limited number of apatite crystals. Nevertheless, the surface bioactivity was increased compared to the uncoated surface since no similar morphology was observed on the uncoated sample surface, besides Si$_3$N$_4$. The mechanism of apatite formation on coated samples after immersion in SBF is based on the growth of these globules in atomic-sized nucleation sites created by the ALD process. In this process, if there are no more available sites for the gaseous precursors to chemisorb, the substrate surface is considered saturated and the reaction self-terminates. Therefore, if the surface is smooth, it is possible to achieve a homogeneous coating. However, in the current samples, rough surfaces might have caused differences in nucleation and crystallization steps.

## Conclusions

In this study, we applied two different ALD cycle ratios, 3:1 and 2:1, of CaO:PO$_4$ on Si$_3$N$_4$ substrates to achieve a thin HAp layer and improve the surface biological properties of Si$_3$N$_4$. Following the coating process, a heat treatment process was applied at 500 °C to achieve a crystalline phase, in line with the literature. The films achieved by the 3:1 ratio were found to be crystalline HAp, and no other crystalline phases were observed by thin film XRD. The characterization

results obtained by EDX and thin film XRD were found to be compatible with minor disparities. Our study has shown that the ALD process followed by heat treatment slightly improved the bioactivity of the surface. It is believed that increasing the number of cycles can lead to a more homogeneous thin coating by slightly increasing the atomic layer thickness, resulting in a more dramatic improvement in bioactivity. The findings of this study may guide research on HAp formation using the ALD process on different substrates.

## Acknowledgments

## References

1. M.J. Hoffmann and G. Petzow, Pure & Appl. Chem. 66[9] (1994) 1807-1814.
2. P. Sajgalik, J. Dusza, and M.J. Hoffmann, J. Am. Ceram. Soc. 78[10] (1995) 2619-2624.
3. H. Kawaoka, T. Kusunose, Y.-H. Choaa, T. Sekino, and K. Niihara, J. Ceram. Process. Res. 2[2] (2001) 51-53.
4. M. Rahaman and W. Xiao, Int. J. Appl. Ceram. Technol. 15[4] (2018) 861-872.
5. Z. Mladenovic, A. Johansson, B. Willman, K. Shahabi, E. Björn, and M. Ransjö, Acta Biomater. 10[1] (2014) 406-418.
6. C.C.G. Silva, O.Z. Higa, and J.C. Bressiani, Mat. Sci. and Eng. C. 24[5] (2004) 643-646.
7. D.J. Gorth, S. Puckett, B. Ercan, T.J. Webster, M.N. Rahaman, and B.S. Bal, Int. J. Nanomedicine 7 (2012) 4829-4840.
8. T.J. Webster, A.A. Patel, M.N. Rahaman, and B.S. Bal, Acta Biomater. 8[12] (2012) 4447-4454.
9. C.C.G. Silva, B. König Jr., M.J. Carbonari, M. Yoshimoto,

S. Allegrini Jr., and J.C. Bressianic, Mater. Charact. 59[9] (2008) 1339-1341.

10. M.P. Arts, J.F. Wolfs, and T.P. Corbin, BMC Musculoskelet Disord. 14 (2013) 244.

11. G. Pezzotti, E. Marin, T. Adachi, A. Rondinella, F. Boschetto, W. Zhu, N. Sugano, R.M. Bock, B. McEntire, and S.B. Bal, Sci. Rep. 7 (2017) 44848.

12. G. Pezzotti, in "Bioceramics" edited by A. Osaka, R. Narayan (Elsevier, 2021) p. 297.

13. M. Vert, Y. Doi, K. H. Hellwich, M. Hess, P. Hodge, P. Kubisa, M. Rinaudo, and F. Schué, Pure Appl. Chem. 84[2] (2012) 377-410.

14. F. Mussano, T. Genova, P. Rivolo, P. Mandracci, L. Munaron, M.G. Faga, and S. Carossa, J. Mater. Sci. 52 (2017) 467-477.

15. M. Hnatko, M. Hičák, M. Labudová, D. Galusková, J. Sedláček, Z. Lenčéš, and P. Šajgalík, J. Eur. Ceram. Soc. 40[5] (2020) 1848-1858.

16. E. Marin, S. Horiguchi, M. Zanocco, F. Boschetto, A. Rondinella, W. Zhu, R.M. Bock, B.J. McEntire, T. Adachi, B.S. Bal, and G. Pezzotti, Heliyon 4 (2018) e01016.

17. E. Salgueiredo, M. Vila, M.A. Silva, M.A. Lopes, J.D. Santos, F.M. Costa, R.F. Silva, P.S. Gomes, and M.H. Fernandes, Diam. Relat. Mater. 17 (2008) 878-881.

18. C.C.G. Silva, E.C.S. Rigo, J. Marchi, A.H.A. Bressiani, and J.C. Bressiani, Mater. Res. 11[1] (2008) 47-50.

19. M. Amaral, A.G. Dias, P.S. Gomes, M.A. Lopes, R.F. Silva, J.D. Santos, and M.H. Fernandes, J. Biomed. Mater. Res. A. 87[1] (2008) 91-99.

20. F. Baino, Materials (Basel). 12[11] (2019) 1754.

21. B.D. Ratner and A.S. Hoffman, Biomaterials Science, 3rd ed. (Academic Press, 2013) p. 259-276.

22. S. Bose, S. Tarafder, and A. Bandyopadhyay, in "Hydroxyapatite (Hap) for Biomedical Applications (Woodhead Publishing Series in Biomaterials, 2015) p. 143.

23. R. Narayanan, S.K. Seshadri, T.Y. Kwon, and K.H. Kim, J. Biomed. Mater. Res. B 85[1] (2008) 279-299.

24. B.A. Jerri Al-Bakhsh, F. Shafiei, A. Hashemian, K. Shekofteh, B. Bolhari, and M. Behroozibakhsh, Bioact. Mater. 4 (2019) 322-333.

25. R. Radha and D. Sreekanth, J. Magnes. Alloy. 8[2] (2020) 452-460.

26. H.A. Siddiqui, K.L. Pickering, and M.R. Mucalo, Materials (Basel) 11[10] (2018) 1813.

27. W.S.W. Harun, R.I.M. Asri, J. Alias, F.H. Zulkifli, K. Kadirgama, S.A.C. Ghani, and J.H.M. Shariffuddin, Ceram. Int. 44[2] (2018) 1250-1268.

28. J. Marchi, C.C.G. Silva, E.C.S. Rigo, A.H.A. Bressiani, and J.C. Bressiani, Abstract book of 11th International Conference on Advanced Materials. 2009.

29. P. Usinskas, Z. Stankeviciute, G. Niaura, J. Maminskas, G. Juodzbalys, and A. Kareiva, J. Solgel Sci. Technol. 83[2] (2017) 268-274.

30. M. Putkonen, T. Sajavaara, P. Rahkila, L. Xu, S. Cheng, L. Niinistö, and H.J. Whitlo, Thin Solid Films 517[20] (2009) 5819-5824.

31. J. Holopainen, K. Kauppinen, K. Mizohata, E. Santala, E.Mikkola, M. Heikkilä, H. Kokkonen, M. Leskelä, P. Lehenkari, J. Tuukkanen, and M. Ritala, Biointerphases 9[3] (2014) 031008.

32. A. Radtke, M. Ehlert, T. Jędrzejewski, B. Sadowska, M. Więckowska-Szakiel, J. Holopainen, M. Ritala, M. Leskelä, M. Bartmański, M. Szkodo, and P. Piszczek, Nanomaterials 9[1] (2019) 123.

33. H. Mandal, F. Kara, A. Kara, and S. Turan, U.S. Patent No. US 7,064,095 B2 (2002).

34. M. Precnerová, K. Bodišová, F. Frajkorová, D. Galusková, Z.V. Nováková, J. Vojtaššák, Z. Lenčéš, and P. Šajgalík, Ceram. Int. 41[6] (2015) 8100-8108.

35. T. Kokubo and H. Takadama, Biomaterials 27[15] (2006) 2907-2915.

36. H.H. Sønsteby, A. Yanguas-Gil, and J.W. Elam, J. Vac. Sci. Technol. A. 38[2] (2020) 020804.

37. G. Carter, Vacuum 56[2] (2000) 87-93.